Appropriate seismic numerical simulation model for the geosynthetic reinforced slope considering boundary effect

Sao-Jeng Chao[1], A. Cheng[1], T.-H. Yu[1], and J. Chao[2]

[1] Department of Civil Engineering, National Ilan University, 1, Shennong Road, Yilan 260, Taiwan.
[2] Department of Civil and Environmental Engineering, University of Massachusetts, Amherst, MA 01003, USA.

ABSTRACT

Geosynthetic reinforced slopes are highly resistant to cyclic stress and earthquakes. Conventional gravity-retaining structures are thus being gradually replaced by geosynthetic reinforced slopoes. Considering the high frequency of earthquakes in Taiwan, earthquake resistance should be taken into account in the design of geosynthetic reinforced slopes to investigate the effects of seismic stress from earthquakes. This study adopted the finite element program Plaxis to simulate the dynamic behaviors of a geosynthetic reinforced slope at FoGuang University, Taiwan. Because dynamic program analysis processes mainly incorporate the earthquake data given in a model, repeated seismic reflections and magnified seismic response can occur within the model boundary when a seismic input is directly applied to the base. Therefore, dynamic boundary conditions provided in Plaxis are applied to simplify the calculation; specifically, applicable boundary conditions for the geosynthetic reinforced slopes may be retrieved using the free-field and viscous boundaries for a dynamic simulation analysis to enhance accuracy.

Keywords: geosynthetic reinforced slope; earthquake; boundary conditions; finite element method.

1 INTRODUCTION

By facilitating interactive behavior between the soil and the reinforced material, geosynthetic reinforced slopes stabilize the soil and resist earth pressure or additional sources of stress from the slope. Because of advantages such as simplicity of application, low cost, short construction duration, adaptability, balanced soil mass distribution, and earthquake resistance, geosynthetic reinforced slopes have been widely applied in slope engineering in Taiwan in recent years, gradually superseding the use of conventional gravity retaining structures.

To examine the influence of seismic force on the dynamic behavior of geosynthetic reinforced soil retaining structures, numerical simulations have been conducted through the finite element method by some researchers (Bathurst and Hatami, 1998; Ling et al., 2009; Liu et al., 2011; Lee and Chang, 2012).

This study investigated the effects of earthquakes on a geosynthetic reinforced slope by installing seismic recording devices to measure the magnitude of ground acceleration. The earthquake data recorded at the demonstration site were used to conduct a FEM analysis with the Plaxis program (Kao, 2014; Wu, 2015). In this paper, the boundary conditions were investigated comprehensively to improve the accuracy of dynamic numerical simulation on seismic behaviors.

2 DEMONSTRATION SITE OF THE GEOSYNTHETIC REINFORCED SLOPE

The slope of the demonstration site was extremely unstable because of previous damage from debris flows caused by typhoons and torrential rain. Considering the hazards of imminent and further damage, this study was conducted after the completion of restoration work. Several earthquake instruments were deployed at the top, middle, and ground portions of the slope (Fig. 1) to explore the various conditions of the geosynthetic reinforced slope under a seismic occurrence.

(a) (b)

Fig. 1. (a) Geosynthetic reinforced slope at FoGuang University; (b) Earthquake monitoring instrument.

The cross-sectional design of the geosynthetic reinforced slope has three portions, with the additional

application of a 200 kN/m reinforced geogrid. The first portion (base structure) of the geosynthetic reinforced slope was designed to be 2.5 m deep, and a six-layer reinforced geogrid was applied, with 0.5 m spacing; the second portion (middle structure) was 15.5 m high with a reinforced slope angle of 45°, and a 51-layer reinforced geogrid was overlaid with 0.3 m spacing; the third portion (top structure) was 12.5 m high with a reinforced slope angle of 73° and a 41-layer reinforced geogrid with 0.3 m spacing. Furthermore, a 2-m-high backfill formation was additionally designed on the top structure of the reinforced slope, which had been previously mixed with cement at an approximately 1.5%-2% weight ratio and processed by compaction after fill up.

After the geosynthetic reinforced slope was established and monitored, a dynamic analysis was conducted using the FEM program in Plaxis with applicable material parameters and applied load settings. Earthquake data recorded on Feb 22, 2014 in the first portion of the geosynthetic reinforced slope was employed in this study for processing through dynamic simulation analysis in Plaxis to obtain the seismic response regarding ground acceleration and the maximum magnification of ground acceleration. The cross-sectional design of the geosynthetic reinforced slope at FoGuang University is displayed as Fig. 2.

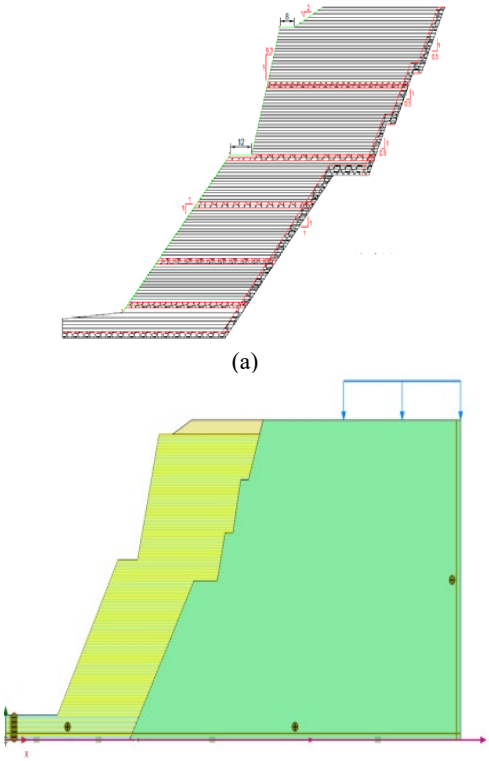

(a)

(b)

Fig. 2. (a) Standard cross-sectional design; (b) Plaxis cross-sectional geometric model.

3 FIELD MONITORING DATA

The earthquake monitoring system in this study observed the seismic activity in the first, second, and third portions, recognizing it through built-in detection technology and recording the data on a host computer. Related seismograph software was used to instantly retrieve data content such as triaxial acceleration and displacement, enabling to provide information for the subsequent dynamic simulation analysis.

According to all the data entries recorded in the earthquake monitoring system since October 2013, most maximum triaxial acceleration responses have had differing magnifications from the first (base structure) to third portion (top structure). Therefore, Data 0222 was adopted as the earthquake input for the dynamic simulation. The maximum acceleration of Data 0222 observed from the first to third portion was 0.092, 0.132, and 0.209 m/s^2, respectively; the magnification ratio detected from the first to second portion was 1.46, whereas the magnification ratio from the first to third portion was identified as 2.25. The seismograph in Fig. 3 represents the seismic activities in the three portions (x = dynamic time, y = acceleration magnitude).

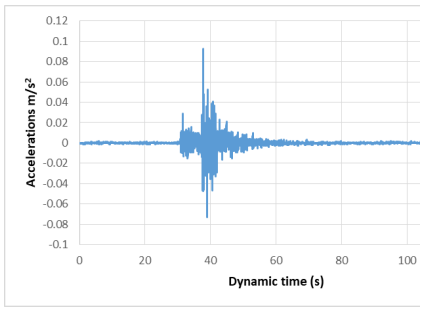

(a)

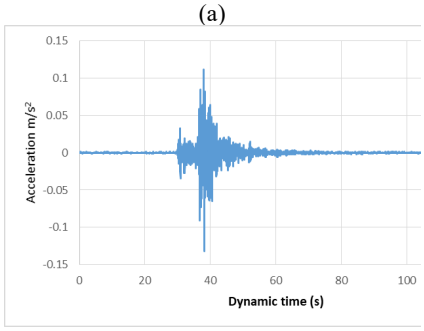

(b)

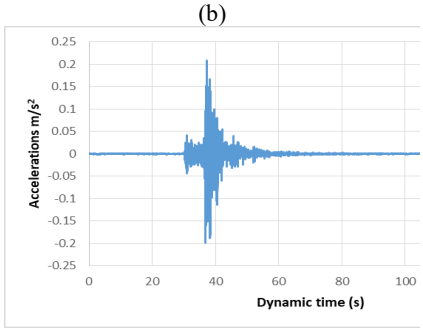

(c)

Fig. 3. Earthquake time history of acceleration observed in field: (a) base structure, (b) middle structure, (c) top structure.

4 PLAXIS FEM ANALYSIS

Plaxis numerical dynamic analysis is used in this study to perform a simulation using specific earthquake data obtained from the recorded data from the site. Inputting seismic waves directly to the base structural layer using fixed boundary conditions can lead to repetitive internal seismic reflection within the model boundary and magnified seismic response. Hence, in a dynamic calculation, the boundary distance should be greater than in the static calculation, considering that the reflection of stress waves can result in imprecise calculations. Because of the additional elements, computing time, and storage demanded for a remote boundary setting, the dynamic boundary condition is required to simplify the calculation process.

Under Plaxis dynamic simulation, viscous and free-field boundary layers can be employed to absorb the reflection of waves. An interface is also required to be created under the model boundary to comply with the boundary conditions and increase simulation accuracy. In this study, a dynamic simulation was conducted using the seismic record of Data 0222. The simulation results were subsequently compared with the corresponding field monitoring records for verification.

4.1 Free-field boundary condition

In the FEM simulations, seismic waves are often inputted horizontally at the base. This study posits that the free-field boundary not only can simulate the response during vibration reception with adequate energy absorption, but the vertical transmission of the seismic response can also be represented. Therefore, the free-field boundary condition can simulate seismic behavior in infinite far-field boundaries to decrease influence from the boundaries and represent actual conditions without generating additional calculations as a result of an enlarged model. In the Plaxis simulation, the free-field boundary conditions can only be applied in lateral boundary conditions (i.e., x_{min} and x_{max}) to simulate the transmission of minimal seismic reflection at far-field boundaries. The modeling of free-field elements was employed laterally at the model boundary and two dampers were additionally deployed in the normal and shear force directions, and with each node positioned at the vertical boundary to absorb wave reflections from the internal structure. A diagram of the free-field boundary [9] is presented in Fig. 4.

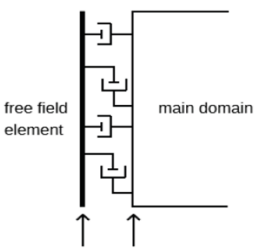

Fig. 4. Energy absorption of the free-field boundary.

4.2 Viscous boundary condition

To eliminate the reflected waves produced in the model interior, the viscous boundary can also be applied to facilitate the absorption of seismic energy, ensuring that the dynamic stimulation can be accurately processed with the model. According to the theory proposed by Lysmer & Kuhlmeyer in 1969, relaxation coefficients c_1 and c_2 should be considered in the Plaxis finite element program if the viscous boundary was assigned based on the bottom boundary of seismic analysis model and subsequently inputted with the earthquake data. The damping absorption of normal and shear force provided by the viscous boundary can be described with the following formula:

$$\sigma_n = -c_1 \rho V_p \dot{u}_x \quad (1)$$

$$\tau = -c_2 \rho V_s \dot{u}_y \quad (2)$$

where

c_1, c_2: absorption coefficient of the viscous boundary
ρ: mass density
V_p, V_S: the velocity of P_ and S_waves
$\dot{u}$: velocity

In addition, because the earthquake data retrieved in this study was entered into the model in only the X direction, the absorption of c_2 was less significant and the results were less affected by the reduction of c_2. Therefore, $c_1 = 1$ and $c_2 = 0.95$ were applied as the parametric hypothesis in the study.

4.3 Predicted results of free-field boundary and viscous boundary dynamic simulation

The free-field and viscous boundary conditions in this study were both used to simulate the dynamic behavior of the geosynthetic reinforced slope. According to the predicted results of the free-field boundary, the earthquake revealed the maximum acceleration value to be 0.098 m/s^2 in the first portion, 0.138 m/s^2 in the second portion, and 0.201 m/s^2 in the third portion. The simulation predicted the ratio of the maximum acceleration between the third and the first portion to be 2.05 or a 3% data error between the simulation and the field monitoring; that between the second and first portion was 1.41 or a 4% data error. The predicted time history of the seismic activity observed in each portion structure are shown in Fig. 5 (X = dynamic time; Y = acceleration).

Alternatively, the dynamic simulation of the viscous boundary identified the maximum acceleration to be 0.090 m/s^2 in the first portion, 0.121 m/s^2 in the second portion, and 0.140 m/s^2 in the third portion. The simulation predicted the ratio of the maximum acceleration between the third and the first portion to be 1.54 or 33% data error between the simulation and the field monitoring; the maximum acceleration between the second and first portions was 1.32 or 8% data error. The time history of the seismic activity observed in each portion structure are shown in Fig. 6.

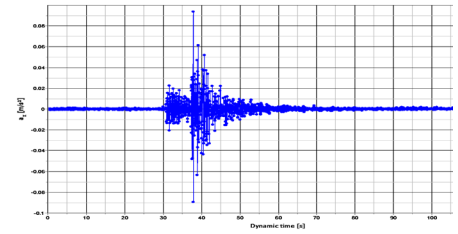

(a)

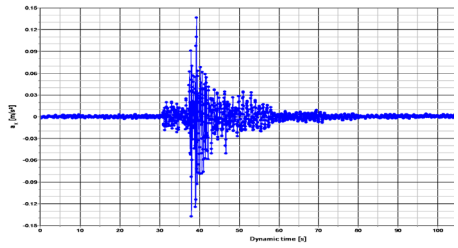

(b)

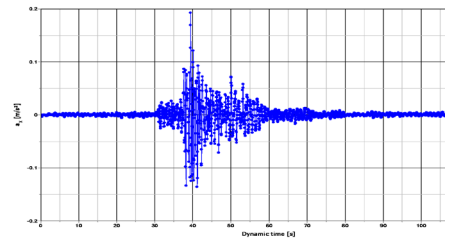

(c)

Fig. 5. Time history of seismic activity in the free-field boundary dynamic simulation: (a) base structure, (b) middle structure, (c) top structure.

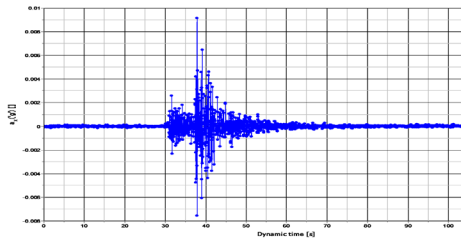

(a)

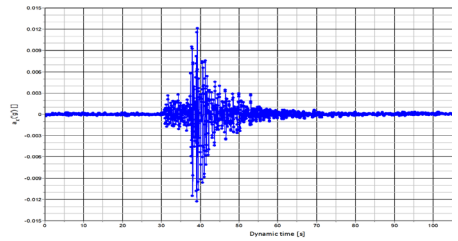

(b)

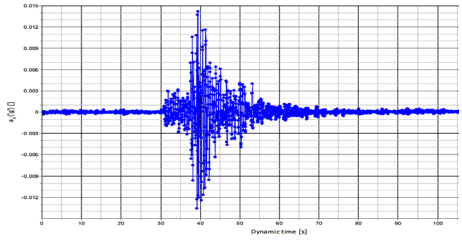

(c)

Fig. 6. Time history of seismic activity in the viscous boundary dynamic simulation: (a) base structure, (b) middle structure, (c) top structure.

5 CONCLUSION

This study organized a geosynthetic reinforced slope for a long-term earthquake monitoring project at FoGuang University, and analyzed the performance of the slope under seismic condition through numerical simulation with the Plaxis finite element program. The earthquake data were retrieved directly from an earthquake monitoring instrument installed at the demonstration site. The data were converted and applied in Plaxis dynamic simulation analysis to examine acceleration status under the seismic forces.

Although the free-field and viscous boundary can both be used to simulate dynamic behaviors in the Plaxis finite element program, these two boundary conditions were compared with the data obtained in the field monitoring. As shown in the simulation results for the maximum acceleration magnification of the free-field and viscous boundaries in the top portion, the maximum acceleration magnification of the third and first portions in the free-field boundary simulation was 2.05, whereas 2.25 was suggested according to the monitoring data; moreover, the maximum acceleration magnification of the second and first portions at the free-field boundary was predicted to be 1.41 in the simulation but was 1.46 in the monitoring record.

The simulation results demonstrated that greater height produces greater effects in the calculation results. Despite free-field and viscous boundaries were both applicable in the dynamic calculation, this study recognized that the free-field boundary was relatively appropriate for the dynamic analysis of goesynthetic reinforced slopes.

REFERENCES

Bathurst, R.J.; Hatami, K. (1998). Seismic Response Analysis of a Geogrid Reinforced Soil Retaining Wall. Geosynthetics International, 5, 1-2, 127-166.

Kao, C.H. (2014). Seismic behavior Monitoring and Numerical Simulation for the Geosynthetic Reinforced Soil Demonstration Site. Master thesis, Department of Civil Engineering National Ilan University.

Lee, K.Z.Z.; Chang, N.Y. (2012). Predictive modeling on seismic performances of geosynthetic-reinforced soil walls. Geotextiles and Geomembranes, 35, 25-40

Ling, H.I.; Leshchinsky, D.; Wang, J.P.; Mohri, Y.; Rosen, A. (2009). Seismic Response of Geocell Retaining Walls: Experimental Studies. Journal of Geotechnical and Geoenvironmental Engineering, ASCE, 135, 515-524.

Liu, H.; Wang, X; Song, E. (2011). Reinforcement load and deformation mode of geosynthetic-reinforced soil walls subject to seismic loading during service life. Geotextiles and Geomembranes, 29, 1-16.

Lysmer, J. and Kuhlemeyer, R. L. (1969). Finite Dynamic Model for Infinite Media. Journal of Engineering Mechanics Division, 95, 859-878.

Wu, R.H. (2015). Study of Appropriate Seismic Numerical Simulation for the Geosynthetic Reinforced Soil. Master thesis, Department of Civil Engineering National Ilan University 2015.